ELSEVIER

Biophysical Chemistry 122 (2006) 206–214

Biophysical Chemistry

http://www.elsevier.com/locate/biophyschem

# Topological and dynamical properties of Azurin anchored to a gold substrate as investigated by molecular dynamics simulation

Anna Rita Bizzarri

*Biophysics and Nanoscience Centre, CNISM, Dipartimento di Scienze Ambientali, Università della Tuscia, I-01100 Viterbo, Italy*

Received 9 January 2006; received in revised form 16 March 2006; accepted 19 March 2006
Available online 28 March 2006

**Abstract**

A classical molecular dynamics study of the electron transfer protein azurin, covalently bound to a gold substrate through its native disulphide group, is carried out at full hydration. With the aim of investigating the effects on the protein structure and dynamics as induced by the presence of an electric field, simulations are performed on neutral, positively and negatively charged substrates. A number of parameters, such as the average structure, the root mean square deviations and fluctuations, the intraprotein hydrogen bonds and solvent accessible surface of the protein, are monitored during 10 ns of run. The orientation, the height and the lateral size of the protein, with respect to the substrate are evaluated and compared with the experimental data obtained by scanning probe nanoscopies. The electron transfer properties between the copper redox center and the disulphide bridge bound to the substrate are investigated and briefly discussed.


*Keywords:* Protein–gold hybrid systems; Molecular dynamics simulation; Azurin; Electron transfer

## 1. Introduction

Understanding of processes associated with proteins bound to surfaces is of fundamental importance in the new field of building hybrid nanodevices [1,2]. The capabilities of biomolecules to perform biological functions, such as electron transfer (ET), catalysis, recognition, can be combined with processing power of microelectronics for the realization of biosensors [3]. In particular, redox metalloproteins, whose activity can be tuned by an external potential, are good candidates for creating hybrid systems [4]. A crucial step in the design of bio-nanodevices is represented by the linkage of proteins to metal substrates with preserved functionality and fast ET rates. In this respect, a direct binding of molecules to electrodes limits the active site-metal distance and could favour an efficient ET rate. To such a purpose, the chemi-adsorption of proteins on gold electrodes can be achieved by exploiting the high affinity of either intrinsic or engineered disulphides and/or thiol groups for gold [5,6]. A wealth of experimental techniques has been applied to investigate the morphological and conductive properties of redox proteins self-assembled on metal electrodes [7–9]. However, a complete picture of the spatial arrangement and the dynamical behaviour of proteins bound to a metal substrate is still far from being reached. In this respect, Molecular Dynamics (MD) simulations could help in the study of the properties of proteins bound to substrates [10–12]. In particular, MD simulated data provide information useful in the analysis of the results obtained by Scanning Tunnelling Microscopy (STM) and Atomic Force Microscopy (AFM) of proteins bound to metal substrates [11,13,14].

To such an aim, we have carried out classical MD simulations of the copper protein azurin (AZ) covalently bound, through its native disulphide bridge, to a flat gold surface, under fully hydrated conditions. Although a complete treatment of the protein–gold interactions requires ab-initio techniques, some relevant, preliminary information can be obtained by a classical approach [13,14]. Furthermore, effects on the protein structure and dynamics as induced by the presence of an electric field, could be evaluated by taking into account positively and negatively charged gold substrates. Such a study offers the possibility to compare MD simulated data with those obtained by STM under an applied voltage bias.

*E-mail address:* bizzarri@unitus.it.

0301-4622/$ - see front matter © 2006 Elsevier B.V. All rights reserved.
doi:10.1016/j.bpc.2006.03.012

AZ is small ET molecule (14.6 kDa for 128 amino acid residues) which acts essentially as an electron carrier in the respiratory chain of denitrifying bacteria. Its structure and dynamics have been well characterized by different experimental techniques [15–18] and also by MD simulations [19]. The active site is asymmetrically located in a hydrophobic core approximately 7 Å from the surface and consists of a single copper ion coordinated to five protein atoms (see Fig. 1); a switching between Cu(I) and Cu (II) oxidation states occurring during the ET process. The exposed disulfide group (Cys3–Cys26), opposite to the copper atom, has been shown to be suitable for covalent linking to gold surfaces via S–Au bonds [20,21]. Indeed, AZ anchored to a gold electrode has gained considerable interest even for its potential application in bio-nanoelectronics [14,22,23]. The morphological, spectroscopic, electrochemical, and ET properties of AZ on gold substrate have been investigated, even in the single molecule limit, by AFM, STM, cyclic voltammentry, ellipsometry and phosphorescence spectroscopy [9,20].

An overview of the structural and dynamical properties of AZ on gold has been provided by monitoring a number of properties, such as the average structure, the root mean square displacements (RMSD), the root mean square fluctuations (RMSF), the protein solvent exposed surface and the spatial arrangement of the copper ion with respect to the gold surface during a run of 10 ns. With the aim of comparing the MD simulation results with the AFM and STM data, the protein has been represented as an ellipsoid whose height and lateral size have been evaluated as a function of the simulation time; these data having been analyzed in connection with experimental data. By taking advantage of the MD simulation approach in sampling configurations of functional relevance for a hybrid system, we have also investigated the ET process occurring from the copper active site to the disulphide bridge anchored to the gold substrate. In particular, the corresponding ET rates have been calculated in the framework of the organic model, treating the protein as a disordered system [24]. The results have been compared and briefly discussed in connection with possible implications for hybrid bio-nanodevices.

## 2. Computational methods

### 2.1. Molecular dynamics simulations

The MD simulations of AZ bound to a gold substrate were performed with CHARMM (version c28b) [25] using CHARMM 27 Force Field [26]. Initial coordinates of AZ were taken from the X-ray structure at 0.193 nm resolution (4AZU, entry of Brookhaven Protein Data Bank) [27]. With the exception of the copper ligands, all the ionizable residues were assumed to be in their fully charged state, according to a pH value of 5.5.

Various models were developed to parameterize the metal–ligand interactions in copper metallo-proteins [28–31]. We were assumed that the AZ copper ion was bound to three ligands (two nitrogen, from His46 and His117, respectively, and one sulphur from Cys112, while the much weaker interactions of copper with the sulphur from Met121 and the carbonyl oxygen from Gly45 were treated by a nonbonded approach [19,32]. The partial charges for the copper and its ligand residues were assigned according to [28]. To model the Au(111) surface, the gold atoms were arranged hexagonally into a cluster of three layers each one made by $22 \times 25$ atoms. The nearest neighbour distance was assumed to be 2.88 Å and the positions of the gold atoms were kept fixed during all the simulations.

A was anchored to the gold surface through the sulphurs of the native disulphide bridge, which was kept linked upon binding to gold. Each sulphur of the bridge was covalently bound to a single gold atom in atop position, approximately placed at the center of the gold surface. Such an approach is

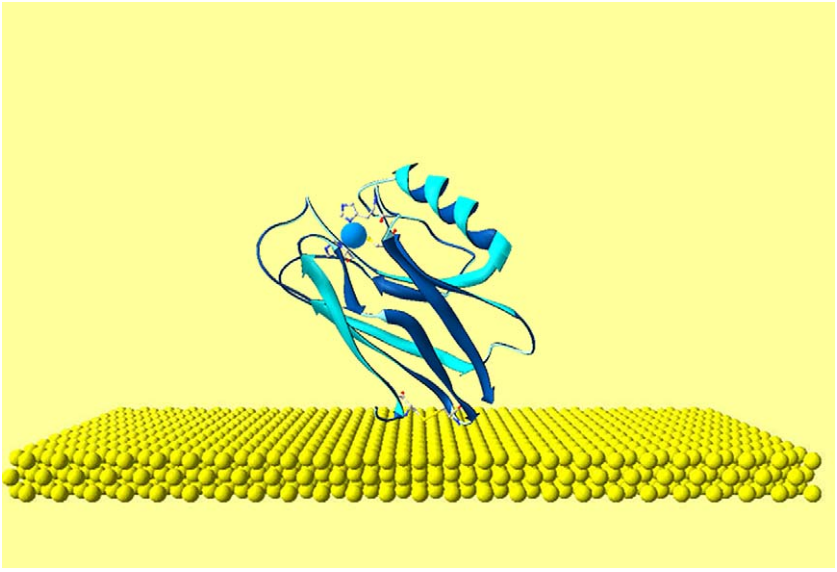

Fig. 1. Starting configuration of AZ, hydrated by 395 water molecules, on Au(111) substrate. AZ is bound to gold through the S–S group of Cys3 and Cys26 (yellow spheres). The copper atom in the active site, opposite to the S–S group, is represented by an orange sphere. (For interpretation of the references to colour in this figure legend, the reader is referred to the web version of this article.)

supported by a recent ab-initio study dealing with the binding of monothiols to gold substrates [33]. The S–Au bond was described by a harmonic bond with a constant of 198 (kcal/mol $Å^2$); for the other parameters see Ref. [11].

The AZ molecule bound to gold was centered in a cubic box of edge 5.6568 nm filled with 5832 water molecules which were modeled by TIP3P force fields [34], equilibrated at 300 K. Then, any water molecule placed from each protein or gold atom at a distance smaller than 0.28 nm and higher than 1.00 nm was removed. The protein charge was balanced by randomly placing two sodium ions to ensure the charge neutrality of the protein–gold system. The final system was constituted of 1643 water molecules and two sodium ions surrounding the AZ molecule, at a hydration level of about 2.0 g of water *per* g of protein, assuring a full biological functionality [35]. The parameters used to describe the Lennard–Jones gold–protein interactions are the same as reported in Refs. [11,13].

Starting from the same initial arrangement of AZ on gold, three different simulations were performed. The first MD simulation was carried out by setting the charge of the gold atoms to zero; such a simulation having been named AZAU0. Then, two simulations were carried out by setting the gold at a negative (AZAUN) and a positive charge (AZAUP). In particular, the charge of each gold atom belonging to the first layer was fixed at $-4.2\cdot10^{-4}$ e, $+4.2\cdot10^{-4}$ e, respectively. These charges approximately give rise to an an electric field of about $5\cdot10^{7}$ V/m in the central region of the substrate where the protein is located; such a value being roughly of the same order of that encountered in STM experiments [36]. Even if the assignment of an uniform charge to the gold substrate represents an approximation of the real situation, it however provides a good starting point to evaluate how a charge distribution can affect the structural and dynamical properties of a protein macromolecule. For comparison, a MD simulation of free AZ, at the same hydration level, was also carried out (free AZ).

For all the simulations, 2000 steps of minimization followed by a heating procedure from 0 K to 300 K with increments of 5 K every 0.2 ps were performed. Subsequently, the system was equilibrated at 300 K for 1 ns. Finally, 10 ns of run by sampling trajectories at intervals of 0.1 ps was performed. The Shake constraint algorithm [37] for all hydrogen and cut off ratios of 11 and 13 Å for the Lennard–Jones and the electrostatic energy functions, respectively, were used. The MD simulations were conducted at constant temperature of 300 K using the Nose–Hoover bath [38].

## 3. Results and discussion

### 3.1. Structural and dynamical properties

Fig. 1 shows a schematic representation of the starting configuration of AZ covalently bound to gold through the native S–S bridge; for clearness water molecules were not represented.

The all-atoms RMSDs from the initial protein structure (after minimization and equilibration), as a function of the simulation time, are shown in Fig. 2, for the three AZ–gold systems and for

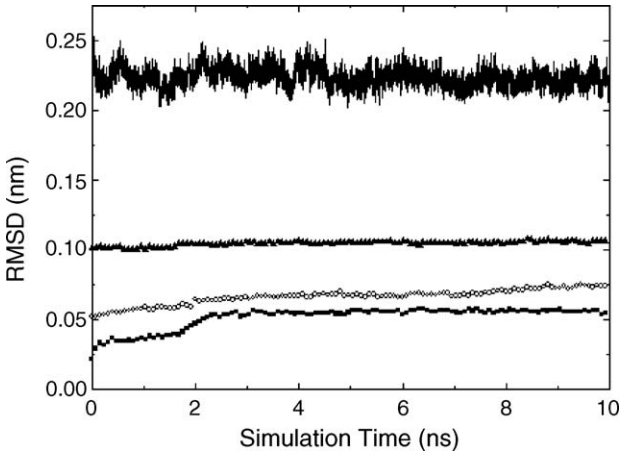


Fig. 2. All atoms RMSD calculated with respect to the initial structure, as a function of simulation time, for AZ bound to neutral, AZAU0 (triangles), positively charged, AZAUP (circles) and negatively charged, AZAUN (squares) substrates; the RMSD of free AZ (continuous line) being also shown. The mean values and the standard deviations of RMSD, as calculated from the (3–10) ns time interval, are: free AZ (0.224±0.007) nm; AZAU0 (0.105±0.002) nm; AZAUP (0.073±0.002) nm; AZAUN (0.056±0.002) nm.

free AZ. The trend in time of the RMSD generally provides some qualitatively and quantitatively information about the departure of the macromolecule from the initial structure in the analyzed temporal window. First, we note that the RMSD values of AZ bound to gold are significantly lower in comparison to free AZ (see Fig. 2 and the average and standard deviation values in the related legend). In addition, a drastic decrease in the temporal oscillations is observed by passing from free to bound AZ molecules; this being more evident for AZ anchored to a charged substrate. Such an effect generally indicates that the anchoring of the macromolecule to a surface by covalent bonds can favour the maintaining of the AZ structure close to its starting configuration. This finds a good correspondence with the results obtained for the RMSD of the copper protein Plastocyanin, similar to AZ, bound to gold. On the other hand, the slightly higher RMSD values obtained for Plastocyanin could be ascribed to the small different structural properties between the two proteins as well as to the different anchoring procedure [11–13].

The observed decrease in the RMSD values by passing from neutral to charged gold points out that the electrostatic interactions between the molecule and its substrate can affect the AZ dynamics. Furthermore, from Fig. 2, it comes out that, while the RMSD is almost constant for AZ on neutral gold, an increasing trend, is registered for the RMSD of AZ on charged surfaces. This can be interpreted as a slowing down of the relaxation of the protein upon binding on gold; i.e. a longer time being required to reach a complete breakdown from the initial structure. In the framework of the Frauenfelder picture, assuming a multi-minima energy landscape explored during the dynamics [39], it can be hypothesized, on one hand a restriction from the AZ molecule, in the sampling of the conformations substates, on the other, a decrease in the kinetics. In other words, a smaller number of accessible substates, local minima of the potential energy hypersurface, are effectively explored by the AZ bound to gold with respect to the free one,

and more slowly. We would like also to remark that the fact that the RMSDs reach, for all the cases, constant values suggests that the system reaches an almost stable configuration in the analyzed temporal window.

The RMSFs as a function of the residue number (see Fig. 3), indicative of the protein flexibility, show smaller values, throughout all the protein residues, for AZ molecules bound to gold with respect to the free protein. It is worth of note that the decrease in the RMSF appears to be different for the various protein regions. The most significant decreases take place mainly at the macromolecular turns, usually characterized by a high mobility. However, a few regions exhibit unchanged, or even enhanced RMSF values. All these results are indicative that the protein flexibility might be affected upon binding the macromolecule to a surface. Such an aspect may have some relevance for the ET properties since the strong interplay between dynamics and functionality. From the general point of view, the evidence that the global dynamics of AZ, anchored to a surface by two atoms, undergoes a significant restriction supports the collective character of protein dynamics [40]. Indeed, a change at a spatially restricted region of the protein might affect the dynamics of the overall protein. Such an aspect deserves also some interest in the applicative use of immobilized proteins whose dynamical behaviour and their functional response might change upon anchoring to a surface. From Fig. 3, we note that the decrease in the RMSF values appears more evident for AZ on charged gold surfaces with respect to AZ on neutral gold with only very tiny differences between positive and negative charged substrates. The presence of charges on the gold surface may give rise to a stronger protein–gold interaction with a decrease of the fluctuation amplitude. Surprisingly, the effect as induced in the protein dynamics upon binding to gold, is rather similar to that occurring when the temperature is lowered [19]. Indeed, in both cases, we observe a restriction in the sampling of the conformational substates.

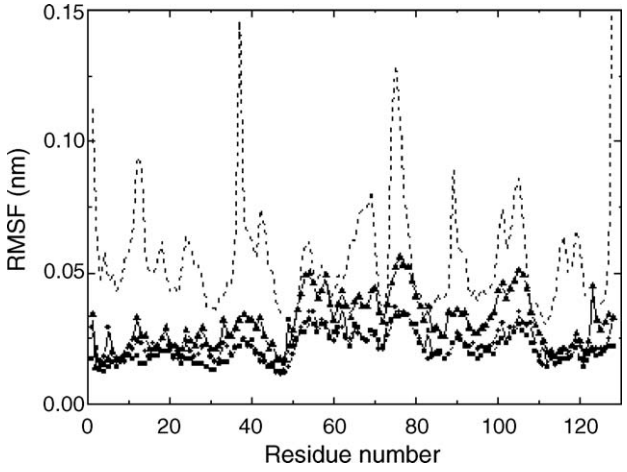


Fig. 3. RMSF of backbone atoms, averaged over 10 ns, for AZ bound to neutral, AZAU0 (Triangles) positively charged, AZAUP, (circles) and negatively charged, AZAUN (squares) substrates; the RMSF related to free AZ being also shown (dashed line).

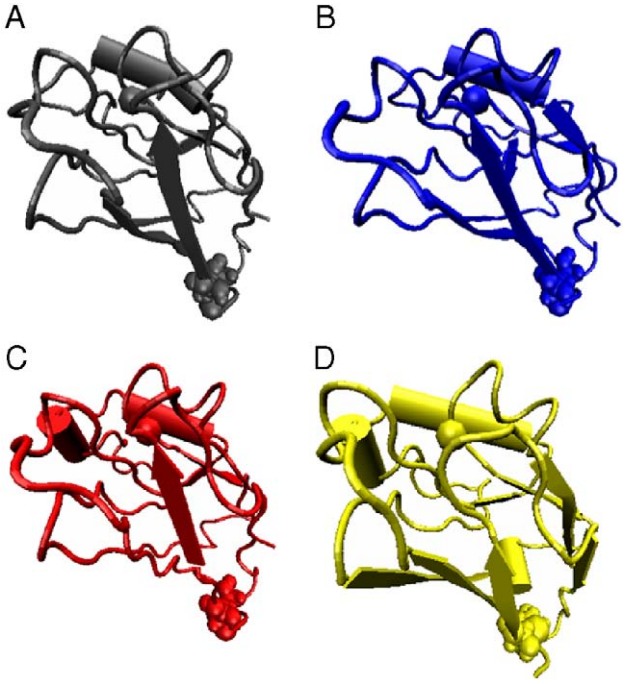


Fig. 4. View of the three average structures of AZ bound to neutral gold, AZAU0, (A grey trace) to positively charged gold, AZAUP, (B blue trace) and to negatively charged gold, AZAU0, (C red trace) and of the average structure of free AZ (D yellow trace); the copper atom and the Cys3 and Cys26 being represented by spheres. The $\beta$-sheet content of the AZ structures is: 31% for free AZ; 23% for AZAU0; 16% for AZAUP; 19% for AZAUN. (For interpretation of the references to colour in this figure legend, the reader is referred to the web version of this article.)

Fig. 4 shows a graphical representation of the average structures for AZ bound to gold and for free AZ. The overall structure is essentially preserved in all the cases, however, some small changes in the AZ secondary structure can be observed. In particular, a small decrease in the $\beta$-sheet content (see the legend of Fig. 4) with a concomitant increase in extent of turn regions occurs in AZ bound to gold; such an effect being more evident for AZ on charged gold substrates. The loss of the secondary structure finds a correspondence in the presence of a lower number of intraprotein H-bonds for AZ on both neutral and charged gold with respect to free AZ (see Table 1). In this respect, we mention that the possibility that a protein macromolecule, located in the proximity of a metal surface, undergoes a protein denaturation, has been suggested by

Table 1
SAS related to the overall protein for the average structures of the three AZ–gold systems and of free AZ (values in parentheses)

| System | Number of intra-protein H-bonds | SAS (Å$^2$) |
|---|---|---|
| AZAU0 AZ on neutral gold (free AZ) | 67 (74) | 6689 (6458) |
| AZAUP AZ on positively charged gold | 62 | 6751 |
| AZAUN AZ on negatively charged gold | 53 | 6812 |

The number of intra-protein H-bonds are also reported.

different experimental approaches (see e.g. Ref. [41]). In particular, Surface Enhanced Raman Spectroscopy has put into evidence the lost of functionality for some redox proteins on metal surfaces [42]. On the other hand, from Table 1, we note that an increase in the Solvent Accessible Surface (SAS) values for AZ bound to gold with respect to free AZ; such an effect appearing more marked for AZ on charged gold. These changes are consistent with the small loss of the secondary structure. On the other hand, since SAS is also strictly connected with the interaction of the macromolecule with its functional partners [44], the possibility that the efficiency of AZ with its partners could be modified should be taken into account. Such an aspect might have some relevance in the use of AZ with their ET partners in hybrid nanodevices. Actually, the small molecular recognition events between AZ bound to gold and cytochrome *c*551 linked to a AFM tip, by Atomic Force Spectroscopy could be ascribed to a reduction of the AZ native form [45].

In summary, AZ bound to neutral and charged gold preserves its global structure with small conformational changes giving rise to a higher exposition of the surface to the solvent with a concomitant decrease in the macromolecular flexibility.

### *3.2. Arrangement of AZ on gold and comparison with scanning probe microscopy data*

To investigate the arrangement of the AZ molecule on gold, we have followed in time the orientation of the virtual *p* axis joining the copper and the sulphur of Cys3 of AZ with respect to the normal of the gold surface. The azimuth and precession angles, $\theta$ and $\Phi$, of the *p* axis are shown in Fig. 5 as a function of simulation time. For all the systems, both $\theta$ and $\Phi$ reveal almost constant values during the simulation time (see also the average and the standard deviation values in Fig. 5). A small increase in both $\theta$ and $\Phi$ is observed passing from neutral to charged gold. This suggests some reassessment in the *p* axis when the protein interacts with a charged substrate. On the other hand, the evidence of small differences in both $\theta$ and $\Phi$, between AZ bound to positively or negatively charged substrates is indicative that the electrostatic interactions could further modulate the arrangements of the macromolecule with respect to the substrate.

Now, we are interested to extract from the MD simulated trajectories information that could be directly compared with experimental topological and morphological data of AZ anchored on gold, as obtained by AFM and STM. AFM provides a good estimation for the height of a protein with respect to the substrate, while it markedly overestimates its lateral size; the latter effect being due to tip broadening effects [9]. On the other hand, STM gives a realistic estimation of the lateral size of a protein on gold; the corresponding macromolecular height being drastically reduced as due to a variety of effects still not well clarified [46]. To compare the MD simulated and scanning probe nanoscopy data, we have introduced a geometric quantity that could well represent the topological properties of a protein over a substrate. The protein has been described as an ellipsoid centered at the center of mass of the protein and oriented as its main inertia axes, according to

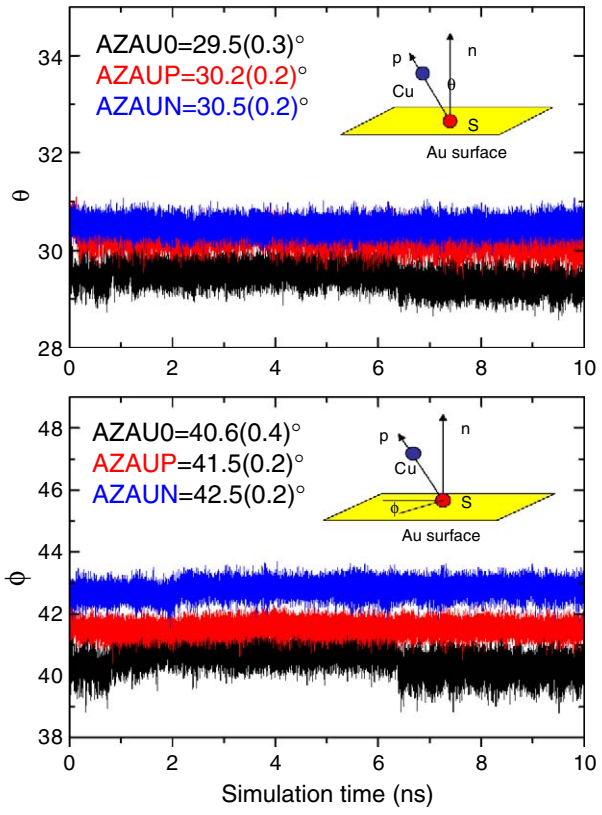


Fig. 5. Temporal evolution, along a 10 ns MD trajectory, of the $\theta$ and $\phi$ angles describing the orientation of the axis joining the copper to and the sulphur of Cys3, with respect to the normal of the gold surface, for the AZ bound to neutral gold (black curve), to positively charged gold (red curve) and to negatively charged gold (blue curve). The average and the standard deviation values are also reported. (For interpretation of the references to colour in this figure legend, the reader is referred to the web version of this article.)

a previously applied procedure [13]. The ellipsoid has been extracted from the MD simulated trajectories by sampling the AZ structures every 10 ps. The corresponding height of AZ over the gold substrate has been evaluated for each ellipsoid structure. The average height values are shown in Fig. 6 for the three AZ–gold systems (see circles). We note that the height values are similar among them and in a good agreement with the value as extracted from the crystallographic structure (3.09 nm) under the assumption of an almost standing up configuration on gold (see Fig. 1). The standard deviation values for all the systems point out that AZ molecules substantially maintain their arrangement on gold during its dynamical evolution; such a finding being in agreement with the small values observed for the $\theta$ and $\Phi$ angles. Notably, higher standard deviations for both $\theta$ and $\Phi$ values were detected for Plastocyanin anchored to gold by a single sulphur of the disulphide group [11,13]. A similar result has been also obtained for yeast cytochrome *c* bound to gold through the thiol from its native cystein [6]. These results find a correspondence with the fact that the macromolecule maintain a higher degree of freedom when it is bound to gold by a single atom.

A slightly lower value for the height of AZ on positively charged gold, in comparison to AZ on neutral and negatively charged gold, is detected. Such a finding suggests that the

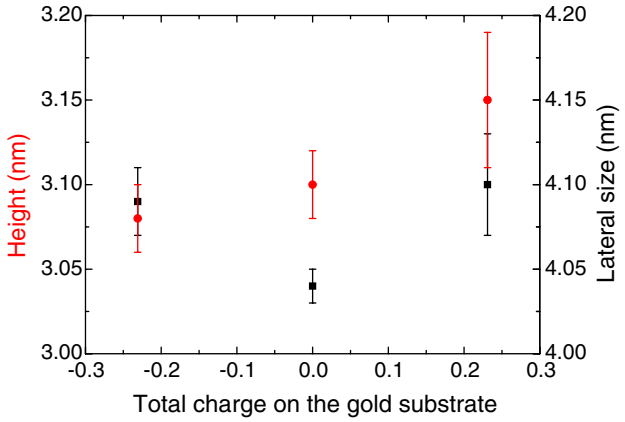


Fig. 6. Height (circles) and lateral size (squares) of the protein structures for the three AZ–gold systems, as extracted from the ellipsoid describing the protein macromolecules during its dynamical evolution (see the text).

presence of charges on gold could weakly modulate the global arrangement of the protein on the substrate. To better understand the role played by the electrostatic interactions in determining the protein arrangement, the distribution of the charges on the AZ external surface on neutral gold has been evaluated. Positively and negatively charged aminoacid residues cover a fraction of 17% and 16% of the total external surface of AZ, respectively; both of them being almost equally distributed over the AZ surface. Such a result suggests a small dependence of the protein height on the presence of charges on gold.

Concerning the AFM measurements of the height of AZ on gold, different sets of values are available in literature [8,9,13]. The work of Davis and Hill put into evidence two populations, one centered at 2.7 nm and another at lower height (1.1 nm) [8]. The first distribution is consistent with a picture in which the protein is anchored by the disulfide bridge in a standing up configuration, the second one suggests a configuration in which the protein is tilted on gold, likely in a denatured form. Other AFM measurements have revealed a single mode distribution centered below 1.7 nm. Again, such a result can be interpreted by assuming that the protein could be partially tilted on gold [13]. On such a basis, the extracted height from MD simulated data for the AZ on neutral gold finds a good correspondence with the experimental AFM data, in which the protein on gold is close to its native form.

Additionally, we note that the AFM experiments show wider distributions ($\sigma$ around 0.6 nm) [8,13] in comparison with that extracted from our MD simulated data. A variety of effects, including a protein–gold interaction more complex than that here accounted for, could really contribute to enlarge the experimental distribution. For example, the stress exerted by the tip on the biomolecule, even in the less invasive tapping mode, the presence of some electrostatic interactions, etc., could affect the experiments [47]. Furthermore, it should be mentioned that AFM data refer to a collection of molecules, which are likely in different starting arrangements; these molecules, highly packed, might also interact among them. Furthermore, AFM and MD simulation data refer to different temporal windows: while AFM measurements occur on a time scale of minutes, MD data covers tenth of nanoseconds.

To estimate the lateral size of AZ on gold, we have projected the ellipsoid on the gold substrate; the diameter by averaging the two axes of the resulting ellipse having been extracted. The average diameter values as obtained by sampling the AZ structure every 10 ps, are also shown in Fig. 6 for the three AZ systems. These values are rather similar among them and in a good agreement with the value (4.2 nm) extracted from the crystallographic structure of AZ on gold in its starting configuration (see Fig. 1), is in agreement with what obtained for AZ height on gold. However, passing from neutral to charged gold, a slight increase of the lateral area is detected; the highest value being registered for AZ on negatively charged gold. The evidence that the widest lateral area is detected in correspondence to the highest height, is indicative that some rearrangement of the protein structure bound to gold occurs. In other words, a small change in the ellipsoid shape is observed when AZ is placed on positively or negatively gold substrates.

Similarly to what observed for the ellipsoid height, rather small values for standard deviations for the lateral area are detected for all the AZ–gold systems. Again, this is indicative of a small variability for the protein arrangement with respect to the gold substrate, in agreement with what observed for $\theta$ and $\phi$.

As already mentioned, the lateral size data of AZ on gold can be compared with the experimental values as extracted by STM measurements which reveal rather homogeneous images with an almost circular shape of radius (4.6±0.7) nm [13]. A good agreement between experimental and MD simulated values for the AZ lateral size is observed. Such an agreement is particularly interesting by taking into account that STM data are collected in the presence of an applied potential between the tip and the electrode, giving rise to an electric field. Therefore, our results suggest that the protein lateral size is not drastically affected under an applied electric field in the range currently used in STM measurements. We remark that the large spread as derived from the STM experimental measurements, similarly to what occur for AFM, arises from a variety of factors whose presence is not accounted for by MD simulations.

### 3.3. Analysis of the ET properties

A crucial aspect of redox proteins bound to a metal substrate is the control of the ET process between the components. Generally, the efficiency of the heterogeneous ET depends on several parameters: distance and orientation of the redox center with respect to the electrode, vibrational coupling, reorganization energy, a full functionality of the biological system, etc. Furthermore, the ET is strongly affected by the properties of the molecule–metal contact; such an aspect being particularly relevant under the application of an electric field to the electrodes [48]. With the aim of qualitatively evaluating the ET properties of upon binding to gold, we have analyzed the ET in terms a semi-classical theory, by neglecting the processes directly involving the molecule–metal interactions. In the weak coupling limit, the

ET reaction rate can be described in the framework of the classical Marcus theory [49]

$$k_{ET} = \frac{2\pi}{\hbar} V_R^2 \left(\frac{1}{4\pi\lambda k_B T}\right)^{1/2} e^{-\frac{(\Delta G^\circ+\lambda)^2}{4\pi\lambda k_B T}} \quad (1)$$

where $V_R$ is the electronic tunnelling matrix element between the donor and the acceptor, $\lambda$ is the reorganization energy ($\lambda$=1.0 eV) for AZ [50] and $\Delta G^\circ$ is the driving force of the reaction; in the activationless limit ($\Delta G^\circ = -\lambda$), the reaction rate, $k_{ET}$, assuming a maximum value.

The dependence of $k_{ET}$ on the medium between the redox centers, to which we are interested, is mainly reflected by $V_R$ expressed by the form:

$$V_R^2 = V_R^{o2} f_M^2 \quad (2)$$

where $V_R^o$ represents the electronic coupling between the redox centers in van der Waals contact, and $f_M$ is a dimensionless attenuation factor which varies between 1 (van der Waals contact) and 0 (infinite distance) [24]. Different approaches have been developed to describe $f_M$ [24,47,51,52]. In the organic model the protein intervening medium is pictured as an organic glass; the random, disordered connections between the donor and the acceptor constituting the overall path of ET [24]:

$$f_M^2 = e^{-\beta R} \quad (3)$$

where $R$ is the distance between the donor and the acceptor centers and the exponential coefficient of decay, $\beta$, quantitatively describes the nature of the intervening medium with respect to its efficiency to mediate ET process. The $\beta$ parameter depends on the protein atom density between the donor and the acceptor [24].

On such a basis, we have evaluated the ET rate from the copper ion (donor) toward the sulphur (acceptor) of Cys3 belonging to the S–S bridge covalently bound to gold for the AZ average structures. The calculation has been performed in the activationless limit that, although it leads to an overestimation of the reaction rate, provides information about the effective coupling between the donor and the acceptor [53]. In Table 2, the distance between the donor and the acceptor, the $\beta$ exponent (see Eq. (3)), the attenuator factors, $f_M^2$, and the related ET rates, as extracted from Eq. (3), applied to the average structures of the AZ–gold systems and of free AZ are reported; the maximum ET rates having been estimated from the expression $k_{ET} \sim 10^{14} f_M^2$. The average donor–acceptor distance is smaller for the AZ molecules bound to gold in comparison to free AZ.

Table 2
Parameters describing the ET process from the copper to the sulphur of Cys3 of AZ average structure, evaluated in the framework of the organic model for the three AZ–gold systems and for free AZ (values in parentheses)

| System | Donor–acceptor distance (Å) | Exponent $\beta$ (Å$^{-1}$) | Attenuator factor $f_M^2 = e^{-\beta R}$ | Maximum ET rate $K_{ET}$ (s$^{-1}$) |
|---|---|---|---|---|
| AZAU0 AZ on neutral gold (free AZ) | 30.12 (27.49) | 1.6963 (1.6475) | $8.1\times10^{-12}$ ($1.510^{-10}$) | $8.1\times10^{2}$ ($1.5\ 10^{4}$) |
| AZAUP AZ on positively charged gold | 30.43 | 1.4232 | $4.0\times10^{-10}$ | $4.0\times10^{4}$ |
| AZAUN AZ on negatively charged gold | 30.45 | 1.5884 | $3.2\times10^{-11}$ | $3.2\times10^{3}$ |

The application of an electric field to an electrode, to which a molecule is bound, could strongly affect its ET properties. Here, we have restricted our analysis to the intramolecular ET, by neglecting the direct metal–molecule processes.

From Table 2, it comes out that no substantial differences in the ET properties occur for AZ bound to positive and negative electrodes. The $\beta$ exponent, related to the atom density between the donor and the acceptor, becomes lower passing from neutral to charged gold systems; the lowest value being detected for AZ on positively charged gold. The $f_M^2$ values, and then the ET rate, as derived for the organic model, are markedly different for the three AZ–gold systems. It is interesting to note that the highest ET efficiency is registered for AZ on positively charged gold, while AZ on neutral gold exhibits the lowest efficiency. This result suggests that the presence of charges on the gold substrate could affect the ET properties of the bound protein. It should be, however, remarked that the obtained maximum $k_{ET}$ is, in all the cases, higher then the experimental value of free evaluated to be 250 s$^{-1}$ [50 as expected since the ET rates have been derived under the activationless limit (see Eq. (2)). A comparison of these results with those of free AZ reveals that both the anchoring to gold and the presence of charges on the substrate can significantly affect the ET rate. Accordingly, the structural changes as induced by the anchoring the protein to a substrate could modulate the functional properties of the macromolecule. Such a finding is particularly rewarding in the evaluation of the efficiency of hybrid bio-devices.

## 4. Conclusions and perspectives

We have applied a classical MD simulation approach to investigate the structure, the dynamics, the arrangement and the ET properties of AZ covalently anchored to a gold substrate through its native disulphide bridge. Our approach provides some preliminary insights on the behaviour of the protein bound to a metal substrate. We have put into evidence a partial denaturation of the protein macromolecule upon binding on gold. Besides offering an overview of changes in both the protein structure and dynamics upon anchoring to a substrate, the MD simulated results could also help in the analysis of the AFM and STM data. Indeed, the height and the lateral size of AZ as derived from the MD simulations can be compared with the available experimental data. Furthermore, the study of the ET properties between the copper and the sulphur bound to gold provides some information about the conductive properties of these systems. Therefore, the capability of MD simulation could be exploited to get insight onto the features of biomolecules assembled on substrates in the perspective to build and improve the electric conduction in hybrid nano-biodevices. Further

developments of the present study might involve a treatment of gold by using polarizable charges and the use of ab initio models for the modelling of the active site and then the ET process.

## References


[1] I. Willner, E. Katz, Integration of layered redox proteins and conductive supports for bioelectronic applications, Angew. Chem., Int. Ed. 39 (2000) 1180–1218.

[2] D.G. Castner, B.D. Ratner, Biomedical surface science: foundation to frontiers, Surf. Sci. 500 (2002) 28–60.

[3] J.S. Marvin, H.W. Hellinga, Conversion of a maltose receptor into a zinc biosensor by computational design, Proc. Natl. Acad. Sci. U. S. A. 98 (2001) 4955–4960.

[4] G. Gilardi, A. Fantuzzi, S.J. Sadeghi, Engineering and design I n the bioelectrochemistry of metalloproteins, Curr. Opin. Struct. Biol. 11 (2001) 491–499.

[5] A. Ulman, Formation structure of self-assembled monolayers, Chem. Rev. 96 (1996) 1533–1554.

[6] B. Bonanni, D. Alliata, A.R. Bizzarri, S. Cannistraro, Topological and electron-transfer properties of yeast cytochrome *c* adsorbed on bare gold electrodes, Chem. Phys. Chem. 4 (2003) 1183–1188.

[7] J. Zhang, Q. Chi, A.M. Kuznetsov, A.G. Hansen, H. Wackerbarth, H.E. Christensen, J.E.T. Andersen, J. Ulstrup, Electronic properties of functional biomolecules at metal/aqueous solution interfaces, J. Phys. Chem., B 106 (2002) 1131–1152.

[8] J.J. Davis, H.A.O. Hill, The scanning probe microscopy of metalloproteins and metalloenzymes, Chem. Commun. 1 (2002) 393–401.

[9] B. Bonanni, D. Alliata, L. Andolfi, A.R. Bizzarri, S. Cannistraro, in: C.P. Norris (Ed.), Surface Science Research Developments, Nova Science Publishers, Inc, 2005.

[10] C.E. Nordgren, D.J. Tobias, M.L. Klein, J.K. Blasie, Molecular dynamics simulations of a hydrated protein vectorially oriented on polar and nonpolar soft surfaces, Biophys. J. 83 (2002) 2906–2917.

[11] A.R. Bizzarri, G. Costantini G, S. Cannistraro, MD simulation of a plastocyanin mutant adsorbed onto a gold surface, Biophys. Chemist. 106 (2003) 111–123.

[12] M. Rief, H.M. Gruebmueller, Force spectroscopy of single molecules, Chem. Phys. Chem. 3 (2002) 255–261.

[13] A.R. Bizzarri, B. Bonanni, G. Costantini, S. Cannistraro, A combined study by AFM and MD simulation of a plastocyanin mutant chemisorbed on a gold surface, Chem. Phys. Chem. 4 (2003) 1189–1195.

[14] J. Zhao, J.J. Davis, M.S.P. Sansom, A. Hung, Exploring the electronic and mechanical properties of protein using conducting atomic force microscopy, J. Am. Chem. Soc. 126 (2004) 5601–5609.

[15] H.B. Gray, J.R. Winkler, Electron transfer in proteins, Annu. Rev. Biochem. 65 (1986) 537–561.

[16] M.A. Webb, G.R. Loppnow, A structural basis for long-range coupling in azurins from resonance Raman spectroscopy, J. Phys. Chem., A 103 (1999) 6283–6287.

[17] E.I. Solomon, M.J. Baldwin, M.D. Lowery, Electronic structures of active sites in copper proteins: contributions to reactivity, Chem. Rev. 92 (1992) 521–542.

[18] A. Paciaroni, M.E. Stroppolo, C. Arcangeli, A.R. Bizzarri, A. Desideri, Cannistraro, Incoherent neutron scattering of copper azurin: a comparison with molecular dynamics simulation results, Eur. Biophys. J. 28 (1999) 447–456.

[19] C. Arcangeli, A.R. Bizzarri, S. Cannistraro, Long-term molecular dynamics simulation of copper azurin: structure, dynamics and functionality, Biophys. Chemist. 78 (1999) 247–257.

[20] E.P. Friis, J.E.T. Andersen, Y.I. Kharkats, A.M. Kuznestov, R.J. Nichols, J.D. Zhang, J. Ulstrup, An approach to long-range electron transfer mechanisms in metalloproteins: in situ scanning tunneling microscopy with submolecular, Proc. Natl. Acad. Sci. U.S.A. 96 (1999) 1379–1384.

[21] L. Andolfi, B. Bonanni, G.W. Canters, M.Ph. Verbeet, S. Cannistraro, Scanning probe microscopy characterization of gold-chemisorbed poplar plastocyanin mutants, Surf. Sci. 530 (2003) 181–194.

[22] P. Facci, D. Alliata, S. Cannistraro, Potential-induced resonant tunneling through a redox metalloprotein investigated by electrochemical scanning probe microscopy, Ultramicroscopy 89 (2001) 291–298.

[23] P.P. Pompa, A. Biasco, R. Cingolani, R. Rinaldi, M.Ph.S. Verbeet, G.W. Canters, Structural stability study of protein monolayers in air, Phys. Rev., E 69 (2004) 032901–032904.

[24] C.C. Moser, J.M. Keske, K. Warncke, R.F. Farid, P.L. Dutton, Nature of biological electron transfer, Nature 366 (1992) 796–802.

[25] B.R. Brooks, R.E. Bruccoleri, B.D. Olafson, D.J. States, S. Swaminathan, M. Karplus, CHARMM: a program for macromolecular energy, minimization, and dynamics calculations, J. Comput. Chem. 4 (1983) 187–217.

[26] A.D.J. MacKerrel, D. Bashford, M. Bellott, R.L.J. Dunbrack, J.D. Evanseck, M.J. Field, S. Fischer, J. Gao, S. Ha, D. Joseph-McCarthy, L. Kuchnir, K. Kuczera, F.T.K. Lau, C. Mattos, S. Michnick, T. Ngo, D.T. Nguyen, B. Prodhom, W.E.I. Reiher, B. Roux, M. Schlenkrich, J.C. Smith, R. Stote, J. Straub, M. Watanabe, J. Wiorkiewicz-Kuczera, D. Yin, M. Karplus, All-atom empirical potential for molecular modeling and dynamics studies of proteins, J. Phys. Chem., B 102 (1998) 3586–3616.

[27] H. Nar, A. Messerschmidt, R. Huber, M. van de Kamp, G.W. Canters, X-ray crystal structure of two site-specific mutants His35Gln and His35Leu of azurin from *Pseudomonas aeruginosa*, J. Mol. Biol. 218 (1991) 427–447.

[28] L.W. Ungar, N.F. Scherer, G.A. Voth, Classical molecular dynamics simulation of the photoinduced electron transfer dynamics of plastocyanin, Biophys. J. 72 (1997) 5–17.

[29] M. van Gastel, W.A. Coremans, H. Sommerdijk, M.C. van Hemert, E.J. Groenen, An ab initio quantum-chemical study of the blue-copper site of azurin, J. Am. Chem. Soc. 124 (2002) 2035–2041.

[30] P. Comba, R. Remenyi, A new molecular mechanism force field for the oxidized form of blue copper proteins, J. Comput. Chem. 23 (2002) 697–705.

[31] O.H.M. Matz, G. Hong G, A. Warshel, Frozen density functional free energy simulations of redox proteins: computational studies of the reduction potential of plastocyanin and rusticyanin, J. Am. Chem. Soc. 125 (2003) 5025–5039.

[32] A.R. Bizzarri, S. Cannistraro, Intensity fluctuations of the copper site resonant modes as studied by MD simulation in single plastocyanin molecule, Chem. Phys. Lett. 349 (2001) 503–510.

[33] D. Fischer, A. Curioni, W. Andreoni, Decanethiols on gold: the structure of self-assembled monolayers unraveled with computer simulations, Langmuir 19 (2003) 3567–3571.

[34] W.L. Jorgensen, J. Chandrasekhar, J.D. Madura, R.W. Impey, M.L. Klein, Comparison of simple potential functions for simulating liquid water, J. Chem. Phys. 79 (1983) 926–935.

[35] J.A. Rupley, G. Careri, Protein hydration and function, Adv. Protein Chem. 41 (1984) 37–172.

[36] O. Marti, M. Amreinm, STM and SFM in Biology, Academ Press, Inc, San Diego, 1993.

[37] J.P. Ryckaert, G. Ciccotti, H.J.C. Berendsen, Numerical integration of the Cartesian equations of motion of a system with constraints: molecular dynamics of *n*-alkanes, J. Comput. Phys. 23 (1977) 327–341.

[38] S. Nose, A molecular dynamics method for simulations in the canonical ensemble, Mol. Phys. 52 (1984) 255–268.

[39] H. Frauenfelder, F. Parak, R.D. Young, Conformational substates in proteins, Annu. Rev. Biophys. Chem. 17 (1988) 451–479.

[40] A.E. Garcia, Large-amplitude nonlinear motions in proteins, Phys. Rev. Lett. 68 (1992) 2696–2699.

[41] A. Otto, What is observed in single molecule SERS? J. Raman Spectrosc. 33 (2002) 593–596.

[42] E.J. Bjerneld, Z. Foeldes-Papp, M. Kaell, R. Rigler, Single-molecule surface-enhanced Raman and fluorescence correlation spectroscopy of horseradish peroxidase, J. Phys. Chem., B. 106 (2002) 1213–1218.

[44] B. Bonanni, A.S.M. Kamruzzahan, A.R. Bizzarri, C. Rankl, H.J. Gruber, P. Hinterdorfer, S. Cannistraro, Single molecule recognition between cytochrome *C* 551 and gold-immobilized azurin by force spectroscopy, Biophys. J. 89 (2005) 2783–2791.
[45] M.L. Connolly, Solvent-accessible surfaces of proteins and nucleic acids, Science 221 (1983) 709–713.
[46] D. Alliata, L. Andolfi, S. Cannistraro, Tip to substrate distances in STM imaging of biomolecules, Ultramicroscopy 101 (2004) 231–240.
[47] J.P. Rossell, S. Allen, M.C. Davies, C.J. Roberts, S.J.B. Tendler, P.M. Williams, Electrostatic interactions observed when imaging proteins with the atomic force microscope, Ultramicroscopy 96 (2002) 37–46.
[48] J. Zhang, M. Grubb, A.G. Hansen, A.M. Kuznetsov, A. Boisen, H. Wackebarth, J. Ulstrup, Electron transfer behaviour of biological macromolecules towards the single-molecule level, J. Phys. Cond. Matter 15 (2003) S1873–S1890.
[49] R.A. Marcus, N. Sutin, Electron transfers in chemistry and biology, Biochim. Biophys. Acta 811 (1985) 265–322.
[50] O. Farver, Y. Lu, M.C. Ang, I. Pecht, Enhanced rate of intramolecular electron transfer in an engineered purple CuA azurin, Proc. Natl. Acad. Sci. U. S. A. 96 (1999) 899–902.
[51] D.N. Beratan, J.N. Betts, J.N. Onuchic, Protein electron transfer rates set by the bridging secondary and tertiary structure, Science 252 (1991) 1285–1288.
[52] W.B. Curry, M.D. Grabe, I.V. Kurnikov, S.S. Skourtis, D.N. Beratan, J.J. Regan, A.J.A. Aquino, P. Beroza, J.N. Onuchic, Pathways, pathway tubes, pathway docking, and propagators in electron–transfer proteins, J. Bioenerg. Biomembranes 27 (1995) 285–293.
[53] M.L. Tan, I. Balabin, J.N. Onuchic, Dynamics of electron transfer pathways in cytochrome *c* oxidase, Biophys. J. 86 (2004) 1813–1819.